

INFLUENCE OF PULSED LASER BEAM HARDENING ON THE FATIGUE LIMIT OF THE STEEL 42CRMO4

T. Hosenfeldt, H. Bomas, P. Mayr

Stiftung Institut für Werkstofftechnik Bremen, Germany

ABSTRACT

In comparison to conventional heat treatments, laser beam hardening has some specific advantages. As a result of the locally limited heat input, the distortion of the material is essentially reduced. Because of the self-quenching process it is possible to abandon cooling agents and additionally laser hardening is well qualified for the integration in automated manufacturing systems. In the field of transformation hardening, Nd:YAG-lasers are superior to CO₂-lasers due to higher energy impact into the material and their greater flexibility. By using pulsed mode, case hardness and case hardening depth are increased. The material is exposed to a rapid thermal cycling during the pulsed laser treatment. The aim of the examinations are the description of the microstructure, the distribution of hardness and residual stress and the resulting fatigue limit in dependence on the laser parameters. On flat bending 42CrMo4 specimens single tracks in longitudinal direction were locally hardened with various laser parameters. The laser pulse frequency was varied between 12.5 Hz and 100 Hz. It has been found, that surface melting causes high roughness, high tensile stresses over the whole track surface and has a detrimental effect on the fatigue limit. Hardening in the solid phase results in high compressive residual stresses in the track and tensile stress peak values in the heat affected zones, a very fine martensitic structure and in comparison to conventional heating higher hardness values.

INTRODUCTION

Laser beam hardening of steel is a surface hardening treatment. The outer material layer is austenitized for a very short time by a laser beam impact which is followed a selfquenching with martensitic phase transformation caused by the cooling capacity of surrounding cold material. The austenitizing temperatures higher than 1000 °C are reached by heating velocities of 10³ up to 10⁶ K/s [1]. The main advantages of Nd:YAG-lasers over CO₂-lasers are due to the smaller wavelength, which makes it possible to renounce on absorption raising coatings and use light-wave cables to guide the laser beam [2]. Bergmann and Lang [3] reported, that pulsed radiation increases the hardness depth over cw-radiation. Frequencies below 50 Hz enhance the risk of surface melting [4]. In practical application components are hardened in areas with high wear rates, to increase the wear resistance [5-12]. The influence of cw-laser beam hardening on the fatigue limit was investigated for unnotched [13-21] and notched [17, 20, 22-25] specimens. Scholtes and Mordike [13] as well as Winderlich and Brenner [16] determined, that transformation hardening with overlapping tracks does not increase the fatigue limit of unnotched specimens. A melted surface while heating entailed a drop in fatigue limit [16]. A favourable influence on the fatigue limit of unnotched specimens was reached by hardening the whole surface with one single track. Winderlich and Brenner [16] measured an improvement of 60 % and Belló et al. [18] of 8 %. An additional hardening with two laser tracks perpendicular to the first implicated tempering effects in the heat affected zone; therefore the fatigue limit traced back to the value of

the base material [18]. Cerny et al. [21] determined a drop in fatigue limit of 16 % after hardening round specimens with single tracks. An area wide hardening with spirally overlapping tracks on round specimens affects an increase of the fatigue limit between 28 and 87 % [14, 15, 17, 20]. The main reason for the increase are compressive residual stresses between -450 and -800 MPa in the laser tracks. The fatigue limit of circumferential-notched round bar specimens was improved between 22 and 115 % if the laser track covered the notch [17, 20, 22, 25].

The present investigations with continuous lasers show, that the fatigue limit decreases in the case of surface melting or if the heat affected zone is overlaid with external load. The fatigue limit can be improved by area-wide hardening and hardening of notches, if compressive residual stresses occur after hardening in the loaded area.

The influence of pulsed laser hardening with Nd:YAG lasers on the residual stress distribution is only insufficiently and on the fatigue not investigated yet and is therefore content of this article.

INITIAL STATE OF THE SPECIMENS

The investigated material was the steel 42CrMo4 (EN 10083) which was delivered in two batches. For the variants hardened with power control batch LV and for the variants hardened with temperature control batch TV was used.

Mechanical properties of the batches were determined by the tensile and hardness tests (Table 1). Flat bending specimens were machined and ground in longitudinal direction (Figure 1a) and compressive residual surface stresses according to Table 1 were achieved. The surface roughness was $R_{y5} = 2.5 \pm 0.5 \mu\text{m}$.

TABLE 1
MECHANICAL PROPERTIES FOR THE QUENCHED AND TEMPERED BASE MATERIALS AND SPECIMENS
(MEAN VALUE AND STANDARD DEVIATION)

batch	$R_{p0.2}$	R_m	A_5	hardness	residual stress	
	MPa	MPa	%	HV0.1	longitudinal MPa	transverse MPa
LV	948 ± 6	1044 ± 10	17 ± 1	318 ± 10	-100 ± 16	-273 ± 7
TV	1107 ± 13	1260 ± 17	13 ± 1	396 ± 6	-118 ± 19	-287 ± 8

LASER TREATMENT

The laser hardening of the specimens was exercised in two ways: All specimens of batch LV were hardened with control of the median power. The laser was a Nd:YAG-laser by type of Lasag KLS 322 with a maximum power output of 300 W. The pulse frequency was varied between 12.5 Hz and 100 Hz. All specimens of batch TV were hardened with control of the peak temperature. The applied laser was a Rofin Sinar CW 020 with a maximum power output of 2 kW. The process parameters are summarised in Table 2, the power controlled variants are described with L and the temperature controlled ones with T. Additionally, the used pulse frequency is indicated.

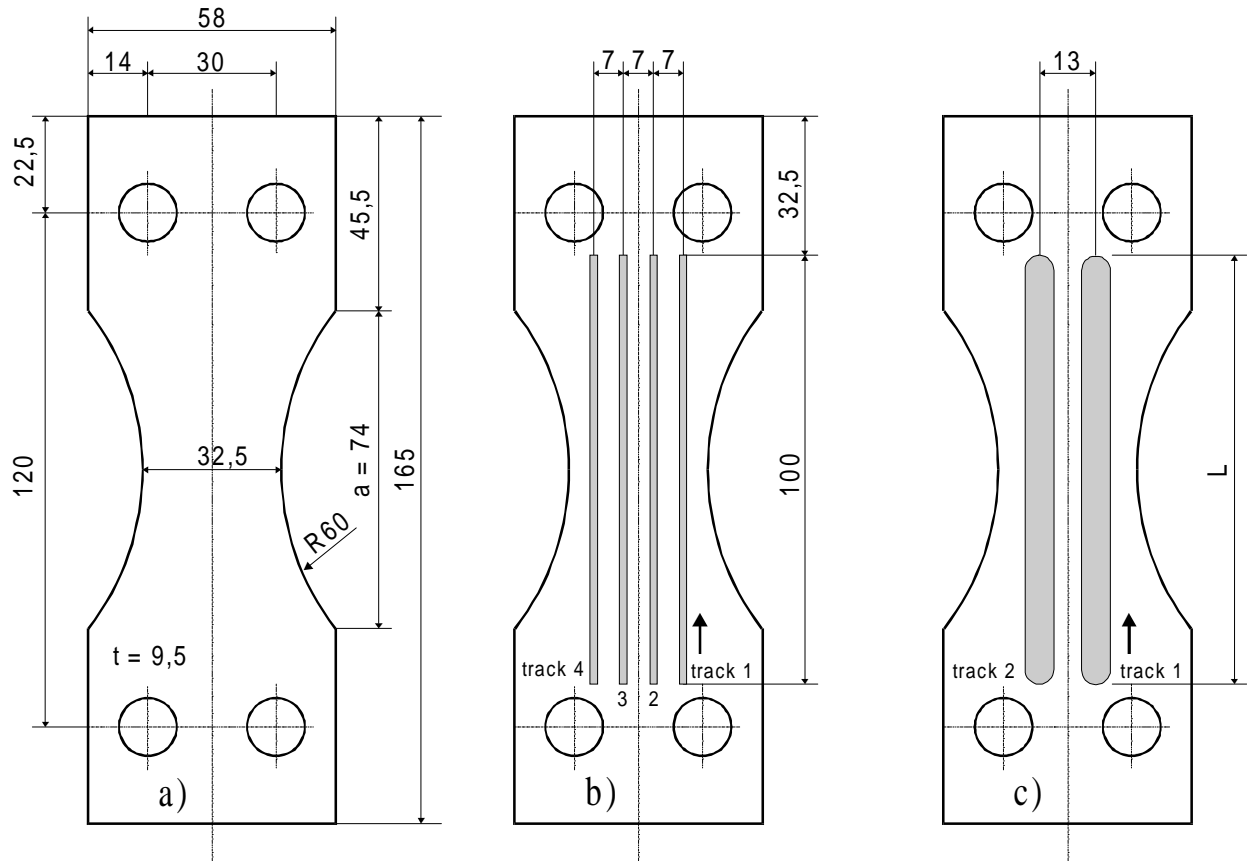


Figure 1: Specimen geometry: a) quenched and tempered, initial state variant, b) variant hardened with power control, c) variant hardened with temperature control

TABLE 2
PROCESS PARAMETERS FOR THE PULSED LASER HARDENING

variant	f_p [Hz]	t_i [ms]	duty cycle [%]	P_{av} [W]	T_c [°C]	v_f [m/min]
L12.5	12.5	4	5	150	-	0.2
L25	25	3	7.5	200	-	0.1
L50	50	2	10	250	-	0.1
L100	100	1	10	250	-	0.1
T25	25	24	60	2000	1350	0.15
T50	50	8	40	3000	1350	0.15
T100	100	4	40	3000	1350	0.15
T100LMW	100	4	40	-	1130	0.15

RESULTS AND DISCUSSION

Hardness and structure

The variants hardened with power control can be classified in two types. First, hardening with surface melting which occurred at small pulse frequencies (L12.5 and L25) and hardening without melting by the use of high frequencies (L50 and L100). The surface of the melted tracks shows a material drive out from the centre with an accumulation at the edges as well as an increase of surface roughness (Figure 2b). The unmelted specimens show a smooth surface. The plateau hardness values are between 606 HV0.1 and 790 HV0.1 (Figure 2a). The melted areas show lower hardness values. The widths of the tracks are about 3 mm and the depths range between 0.15 mm and 0.32 mm. From the hardened zone to the bulk material the hardness drops with a steep gradient. In the melted area the material shows a dendritic solidification structure (Figure 3a).

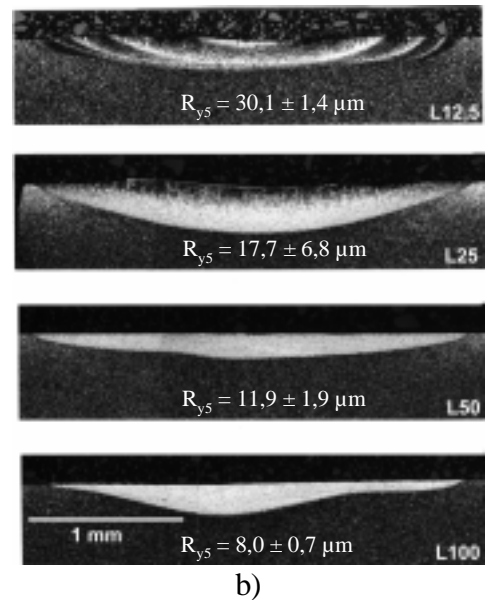
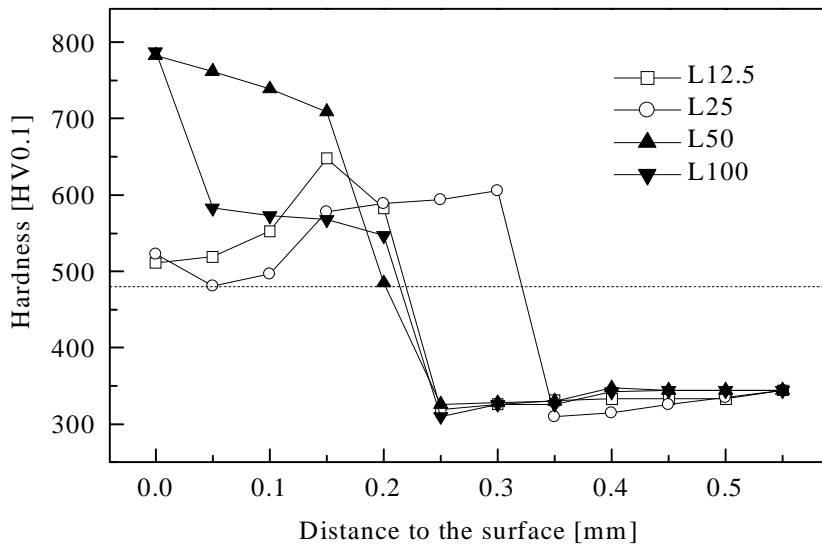


Figure 2: a) Hardness profiles and b) microstructures of the power controlled hardened specimens

In Figure 3b the microstructure of a melted (L25) and a solid phase transformed variant (L100) is shown.

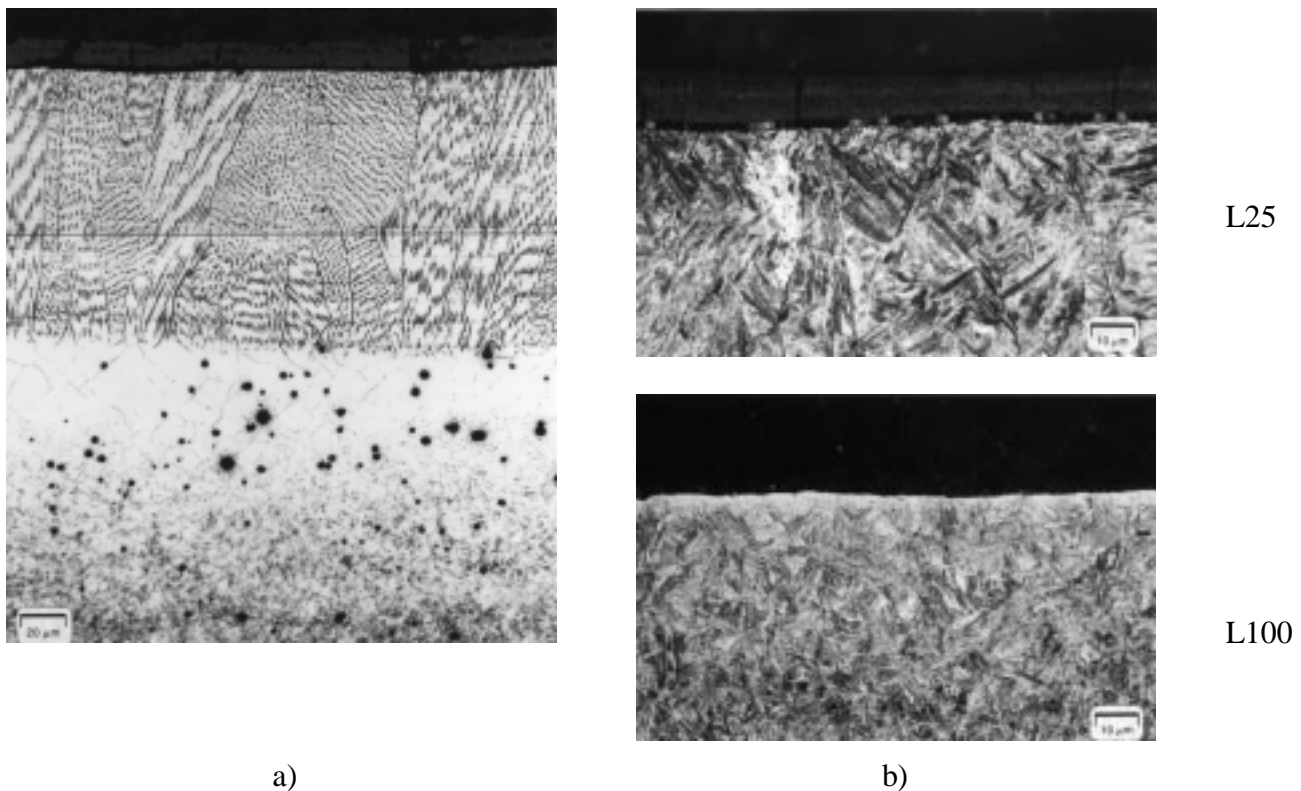


Figure 3: a) Dendritic solidification structure of the melted variant L25; b) microstructure for the variants L25 and L100

Starting with a grain size of 11 from the bulk material, the grain size decreases to 13 at the transition to the hardened zone. The minimum grain (ASTM 14-15) size is reached in the part of the hardened area with the maximum distance to the surface. Due to higher austenitizing temperatures, the grain size increases with decreasing distance to the surface. The size of the austenite grains correlates with the size of the martensite plates. Hardening without melting results in a very fine martensitic structure, the melted areas show a comparatively coarse structure with bainitic parts. The maximum hardness values of the temperature controlled specimens range between 719 and 779 HV0.1 (Figures 4a and 5a). At the transition zone from the hardened material to the base-material the hardness drops rapidly. In the heat affected zone surrounding the hardened track the hardness is less than in the base material. Because of the higher laser power in comparison

with the temperature controlled experiments a larger volume was transformed. The track width ranges between 7.1 (T25) and 8.0 mm (T100LMW), the depth is about 1.4 mm.

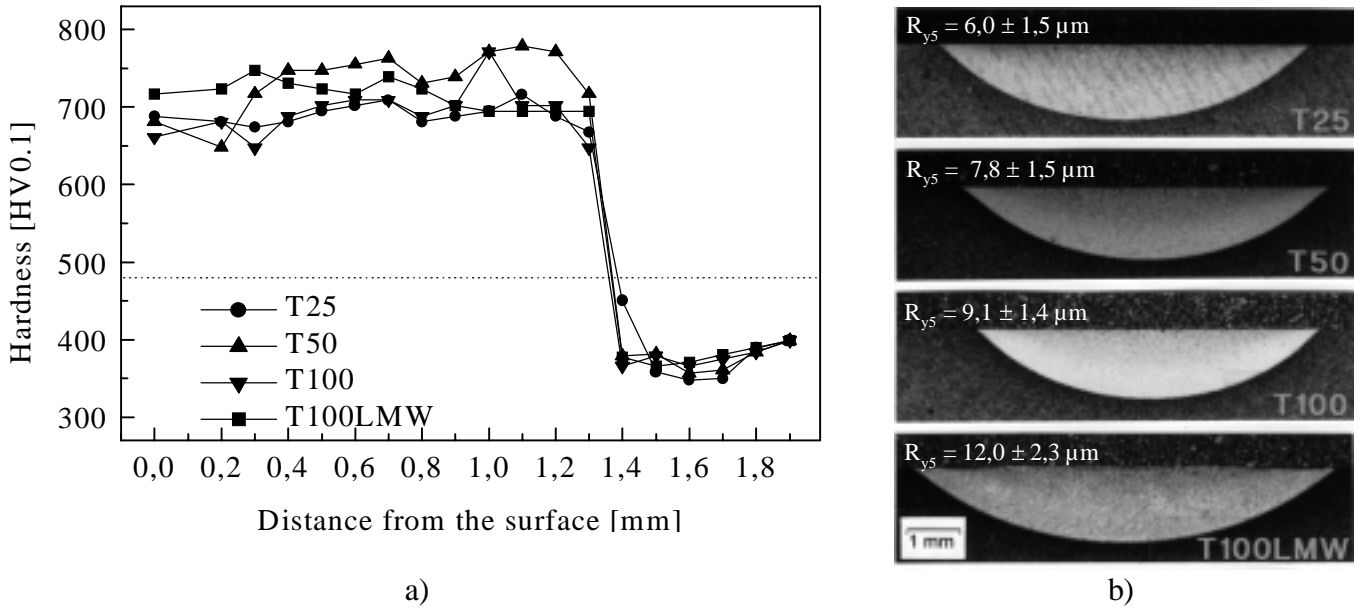


Figure 4: a) Hardness profiles and b) microstructures of the temperature controlled hardened specimens

Under temperature control, it was achieved to harden with low pulse frequencies without surface melting. Figure 4b shows the smooth surface of specimen T25 with low roughness. The minimal grain size of 14 is reached in a depth of 1000 μm under the surface. At the surface a grain size of 8 was measured in the track centre. The grain size declines to the edges to 13 due to the higher austenitizing temperatures and higher cooling rates.

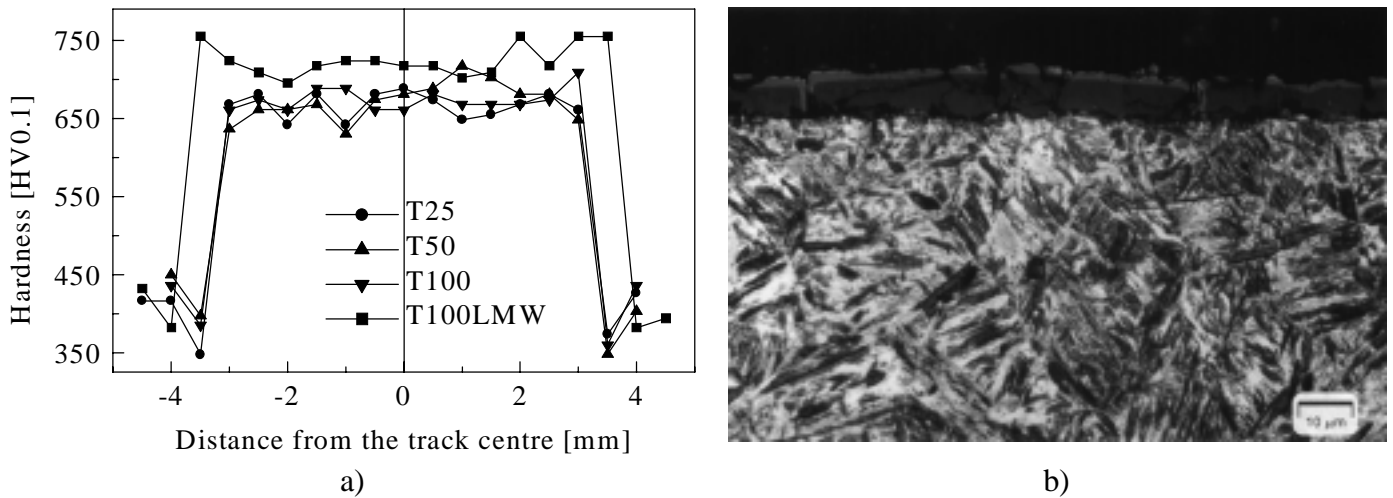


Figure 5: a) Hardness profiles at the surface across the temperature controlled hardened tracks; b) microstructure for the variant T25

Residual stresses

Residual stresses were measured with X-ray diffraction at the surface in intervals of 0.5 mm. The measurements were evaluated according to the $\sin^2\psi$ -method [26]. At the specimen surfaces a two-dimensional residual stress is existent with the main stresses in longitudinal and transverse direction. Figure 6 shows the longitudinal residual stresses measured across the track surfaces. The residual stress distribution of the specimens hardened with power control show two different types. Surface melting induces tensile residual stresses in the whole track surface (L12.5 and L25). Specimens without melting show an M-shaped residual stress distribution with tensile peak values in the heat affected zones and transformation induced compressive residual stresses across the track with peak values at the edges. The transverse residual stresses are qualitatively comparable to the longitudinal ones. The specimens hardened with temperature control show a

W-shaped residual stress curve with tensile peak values in the heat affected zones and compressive values in the track which decrease to the centre (Figure 6b). With respect to the larger transformed volume the compressive stresses of the specimens hardened with temperature control reach higher values and a larger area respectively volume shows compressive residual stresses. The distributions of the transverse residual stresses show lower tensile stress values and higher compressive stresses. After removing of surface layers the gained residual stress depth profiles showed, that compressive stresses exist throughout the unmelted hardened zone. High tensile stresses, between 505 and 646 MPa, were measured in the heat affected zone under the track.

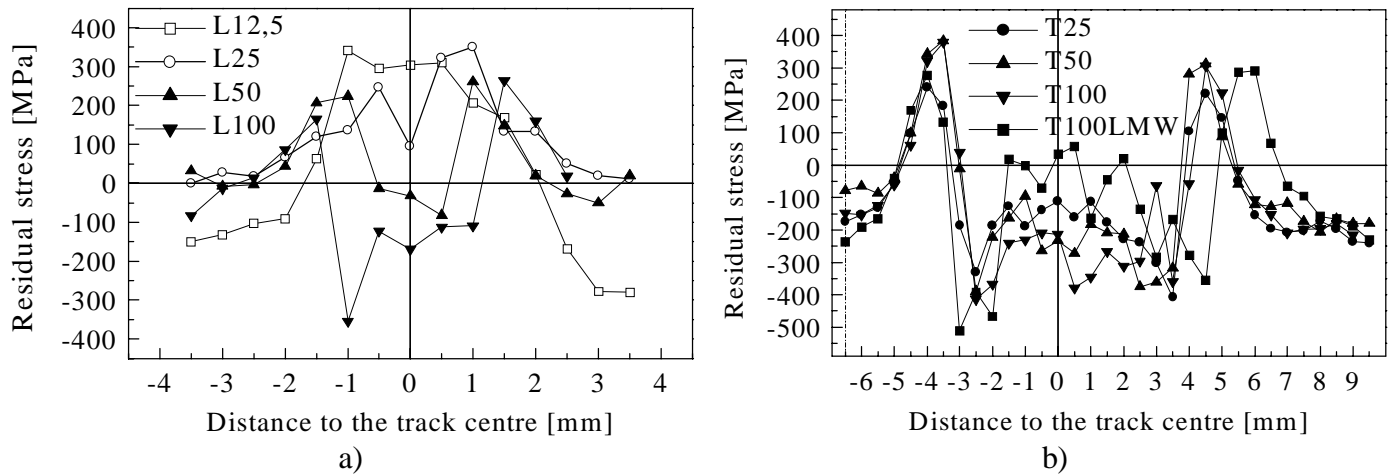


Figure 6: Longitudinal residual stresses at the surface of the hardened track
a) hardened with power control and b) hardened with temperature control

FATIGUE LIMIT

The fatigue tests were carried out under four-point bending with a stress ratio of 0.1. Thus only the laser hardened side was loaded with tensile stress. The results are summarised in Figure 7. The fatigue limit of the base material for the power controlled hardening LV is 398 MPa and for the temperature controlled hardening 404 MPa. Hardening with a liquid phase occurrence has a detrimental effect on the fatigue limit. The variant L12.5 has a fatigue limit of 339 MPa and the variant L25 of only 232 MPa. Hardening in the solid phase influences the fatigue limit not significantly, between -8% and $+2\%$.

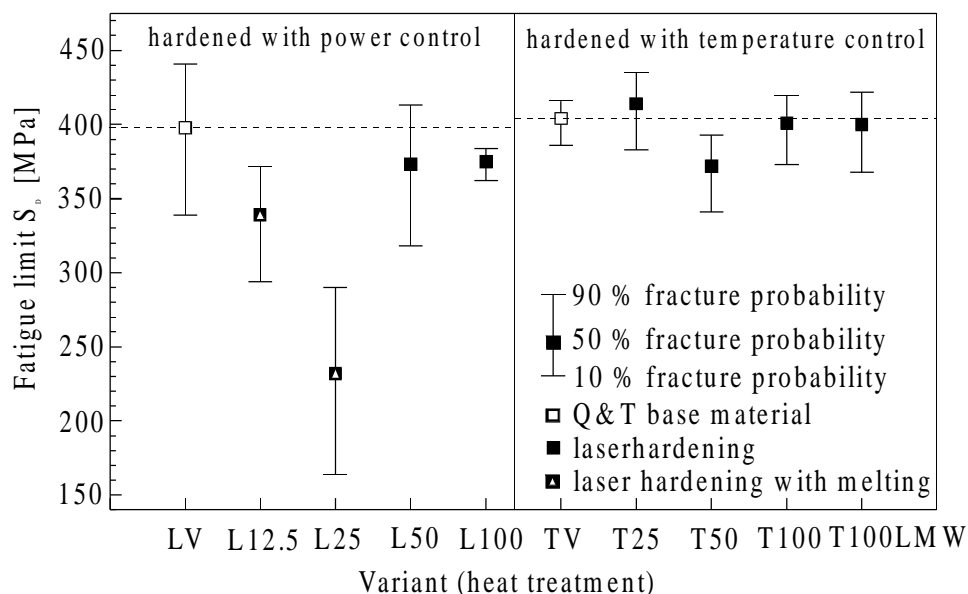


Figure 7: Influence of the pulsed laser hardening on the fatigue limit

Under all conditions the fatigue cracks initiate at the surface. The site of crack initiation of the tempered specimens (LV and TV) is always at the edge of the waist. In the case of surface melting the cracks initiate in the track, a location with high tensile residual stresses, high roughness and a small crack resistance as a result of the dendritic solidification structure (Figure 8a). Otherwise the cracks start in the heat affected zone neighbouring to the tracks, a location with high tensile residual stresses and low hardness (Figure 8b).

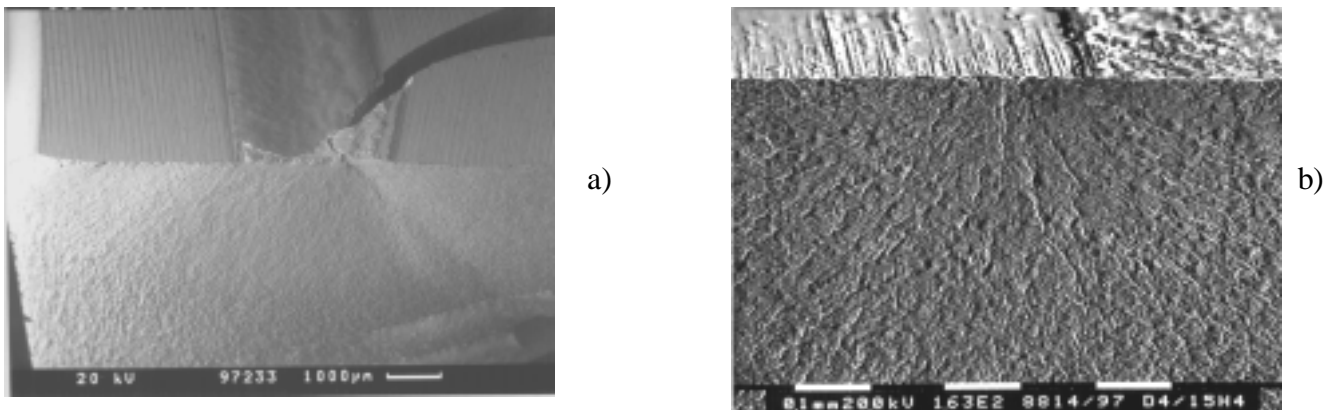


Figure 8: Fracture faces: a) crack initiation inside the hardened track in case of surface melting, b) crack initiation in the heat affected zone in the heat affected zone next to the track

SUMMARY

The influence of pulsed laser beam hardening of tracks in load direction on the fatigue behaviour of the steel 42CrMo4 was investigated. In the first project section the laser hardening was controlled with the median power. The distance between the tracks was so large that no tempering effect of the previous track was determined. With the power controlled process surface melting was inevitable at low pulse frequencies whereby the fatigue limit decreased by 15 % till 42 %. In that case, fatigue cracks initiate on the laser hardened track surface, a location with high tensile residual stresses, high roughness and a small crack resistance as a result of the dendritic solidification structure. In the second section the laser hardening was controlled by the peak temperature. Under these conditions it was possible to harden with a low pulse frequency of 25 Hz without surface melting. In the case of hardening without the occurrence of the liquid phase, compressive residual stresses are measured inside the transformed volume and tensile stresses in the heat affected zone. The influence on the fatigue limit is between -8% and $+2\%$. The fatigue cracks start always at the heat affected zone next to the track at the surface, where high tensile residual stresses and low hardness values exist. The investigations showed, that it is possible to produce locally hardened areas on flat specimens with a pulsed Nd:YAG-laser to improve the wear resistance without a decrease in fatigue strength.

ACKNOWLEDGEMENTS

This work was supported by the “Deutsche Forschungsgemeinschaft (DFG)” under contract number MA 937/40. The laser hardening was done by the “Bremer Institut für angewandte Strahltechnik (BIAS)”, the variant T100LMW was hardened at the “Lehrstuhl Metallische Werkstoffe” in Bayreuth.

REFERENCES

- 1) Meyer-Kobbe, C. (1990). Doctoral thesis, Universität Hannover.
- 2) Wissenbach, K.; Vittr, G. (1995). In: *Präzisionsbearbeitung mit Festkörperlasern*, pp. 274-298, VDI-Technologiezentrum Physikalische Technologien (Eds)., VDI-Verlag, Düsseldorf.
- 3) Bergmann, H. W.; Lang, A. (1993). In: *Präzisionsbearbeitung mit Festkörperlasern*, VDI-Technologiezentrum Physikalische Technologien (Eds). VDI-Verlag, Düsseldorf.
- 4) Messer, K.; Bergmann, H. W. (1997). *Härterei-Technische Mitteilungen* 2, 74.

- 5) Miller, J. E.; Wineman, J. A. (1977). *Metal Progress* **5**, 38.
- 6) Amende, W.; Zechmeister, H. (1982). *VDI-Zeitschrift* **124**, 581.
- 7) Strong, G. J. (1983). *Laser Focus/Electro-Optics* **Nov.**, 172.
- 8) Belforte, D. A. (1984). *Laser News* **Sept.**, 6.
- 9) Paul, H.; Pollack, D. (1986). *Neue Hütte* **31**, 426.
- 10) Mandziej, S.; Seegers, M. C.; Godijk, J. (1989). *Materials Science and Technology* **5**, 350.
- 11) Bach, J.; Damaschek, R.; Geissler, E.; Bergmann, H. W. (1991). *Härtereitechnische Mitteilungen* **2**, 97.
- 12) Zhang, X. M.; Man, H. C.; Li, H. D. (1997). *Journal of Materials Processing Technology*, **69**, 162.
- 13) Scholtes, B.; Mordike, B.L. (1987). In: *Residual Stresses in Sciences and Technology*, pp. 655-662, Macherauch, E. and Hauk, V. (Eds). DGM, Oberursel.
- 14) Shur, E. A.; Voinov, S. S.; Kleshcheva, I. I. (1982). *Metal Science and Heat Treatment* **25**, 341.
- 15) Singh, E. A.; Copley, S. M.; Bass, M. (1981). *Metallurgical Transactions A*, **12A**, 138.
- 16) Winderlich, B.; Brenner, B. (1988). *Härtereitechnische Mitteilungen* **4**, 229.
- 17) Lin, R. (1992). Doctoral thesis, University Linköping.
- 18) Belló, J. M., Fernández, B. J., Lopez, V., Ruiz, J. (1994). *Journal of Material Science* **29**, 5213.
- 19) Stamm, H.; Holzwarth, U.; Boerman, D. J.; Dos Santos Marques, F.; Olchini, A.; Zausch, R. (1996). *Fatigue & Fracture Engineering Materials & Structures*, **8**, 985.
- 20) Cruz, P. de la; Oden, M.; Ericsson, T. (1998). *International Journal of Fatigue* **5**, 389.
- 21) Cerny, I.; Fürbacher, I.; Linhart, V. (1998). *Journal of Materials Engineering and Performance* **7**, 361.
- 22) Sun, Y.-T.; Li, J.-Q.; Lu, J. (1988). In: *Int. Power Beam Conference: Power Beam Processing*, pp. 191-197, Metzbowler, E. A. and Hauser, D. (Eds). ASM, Metals Park, OH.
- 23) Gusenkov, A. A.; Petrova, I. M.; Polyakov, A. N. (1989). *Proc. of the Int. Conf. on Fatigue of Materials and Structures*, National Research Institute for Materials, Prague, 376.
- 24) Changchun, L.; Xiping, L.; Guangxia, L. (1990). *Engineering Fracture Mechanics* **36**, 9.
- 25) Merrien, P.; Lieurade, H. P.; Theobalt, M.; Baudry, G.; Puig, T.; Leroy, F. (1992). *Surface Engineering* **8**, 61.
- 26) Macherauch, E.; Müller, P. (1961). *Zeitschrift für angewandte Physik* **13**, 305.

SYMBOLS

A_5	[%]	fracture strain
cw	-	continuous wave
f_p	[Hz]	laser pulse frequency
P_{av}	[W]	median laser power
P_H	[W]	laser pulse power
R_m	[MPa]	tensile strength
$R_{p0.2}$	[MPa]	yield strength
R_{y5}	[μm]	surface roughness
S_D	[MPa]	fatigue limit
t_1	[ms]	laser pulse length
T_C	[$^{\circ}\text{C}$]	control temperature
v_f	[m/min]	feed velocity